Investigation of scattering between mirror nuclei ^{7}Be and ^{7}Li

S. Barua,[1] J. J. Das,[2] A. Jhingan,[2] N. Madhavan,[2] T. Varughese,[2] P. Sugathan,[2] K. Kalita,[3] S. Verma,[3] B. Bhattacharjee,[1] S. K. Datta,[2] and K. Boruah[1]

[1]*Department of Physics, Gauhati University, Jalukbari-Guwahati 781014, India*

[2]*Nuclear Science Center, Post Office Box 10502, Aruna Asaf Ali Marg, New Delhi 110067, India*

[3]*Department of Physics and Astrophysics, Delhi University, New Delhi 110007, India*

(Received 17 July 2004; published 13 October 2005)

Angular distribution for ^{7}Be + ^{7}Li elastic scattering has been measured using a ^{7}Be radioactive beam at the Nuclear Science Center, New Delhi, at $E_{\mathrm{c.m.}} = 9.87$ and 8.87 MeV. A compact and highly efficient detector system in kinematic coincidence mode and an in-vacuum target transfer system have been developed to minimize contributions from unwanted channels. The angular ranges covered were $\theta_{\mathrm{c.m.}} = 42^{\circ}$–$66^{\circ}$ and $\theta_{\mathrm{c.m.}} = 114^{\circ}$–$138^{\circ}$. At the backward angles at both energies, the experimental angular distribution shows higher cross sections than the theoretical predictions for the direct elastic channel alone. The experimental data could be fitted with an isospin-dependent complex potential that is analogous to the Lane potential. A coupled-channel calculation with ground-state reorientation could also fit the data.

DOI: 10.1103/PhysRevC.72.044602 PACS number(s): 25.60.Bx, 24.10.Ht, 25.60.Lg, 25.70.Kk

I. INTRODUCTION

Study of scattering of mirror nuclei provides some unique information. Since the odd-A mirror nuclei have similar inner structure, being different only in their valence nucleons, a direct scattering measurement may yield information on the interactions among the valence nucleons. For example, the exchange interaction between the valence nucleons may be estimated from this kind of measurement.

Exchange of valence nucleons in scattering between neighboring nuclei with similar cores had been predicted [1] and also experimentally verified [2]. The "elastic exchange" of nucleons or clusters of nucleons between two colliding nuclei differing by a single nucleon or a cluster (e.g., (^{12}C,^{13}C) [3] and (^{12}C,^{16}O) [4]) has been observed experimentally. Imanishi and von Oertzen [5] explained these "elastic exchanges" in terms of dynamic molecular orbital theory, which was successfully employed for the explanation of the exchange reactions in the atomic domain. They also pointed out the possibility of exchange of valence nucleon(s) between two identical cores. For this kind of elastic transfer, the weaker the particle is bound to the core and the smaller is its mass, the stronger is the exchange interaction [2].

It has been predicted that at low energy, when it is energetically less probable to excite accessible, nonelastic channels, the interaction between the mirror pair may lead to resonant charge exchange [6]. Resonant charge exchange between a nucleon and a nucleus is an experimentally established phenomenon [7–9]. From the study of (p, n) and (^{3}He,^{3}H) reactions it was found that as the mass of the projectile increases, the effect of charge exchange decreases and becomes difficult to measure. However, no systematic study of the charge exchange reaction for higher mass projectiles has been done.

The charge exchange reaction between mirror nuclei is an interesting phenomenon because in the final state, the target and the projectile simply interchange their identity. Also, it is experimentally challenging because final products are indistinguishable from the elastically scattered particles. Because of the antisymmetry effect, the charge exchange reaction cross section is symmetric around 90°. This property ensures that, at least at the backward angles in the c.m., the effect of the charge exchange reaction can be observed in the elastic angular distribution as the elastic cross section is low there.

Measurement of scattering between mirror nuclei is experimentally difficult as it involves radioactive ion beams. To our knowledge, the only scattering of mirror nuclei studied so far is in the systems ^{3}H + ^{3}He [10] and ^{13}N + ^{13}C [11]. The intermediate-mass mirror system ^{7}Be + ^{7}Li between these two systems has been also investigated [12] to check the predicted resonant charge exchange reaction [6]. However, no definite conclusions could be drawn from that experiment. In ^{13}N + ^{13}C scattering it was observed that the cross section showed a rising and oscillating behavior at backward angles at an incident energy of twice the Coulomb barrier. The normalized cross section rises almost up to the Rutherford cross section value. The theoretical calculation for the ^{13}N + ^{13}C system including charge exchange and direct elastic scattering by Kruppa *et al.* [13] also predicted the rise and strong oscillation at backward angles owing to the strong interaction between the valence proton and neutron.

The ^{7}Be and ^{7}Li ground states have been fairly well described by cluster wave functions [14]. ^{7}Be and ^{7}Li are considered as ^{4}He + ^{3}He and ^{4}He + ^{3}H clusters. The binding energy of the clusters to the core is comparable to the binding energy of the last nucleons in these nuclei. However, the probability of cluster exchange (^{3}He,^{3}H) should be smaller than for (p, n) exchange because the exchange probability decreases with mass of the exchanging particles [2].

π + ^{15}N scattering at low energy also showed backward peaking in angular distribution [15]. But in the nuclear medium such features may be less prominent owing to Pauli blocking and absorption. The energy dependence of the charge exchange reaction at low energy for π + ^{7}Li scattering was studied by Irom *et al.* [16].

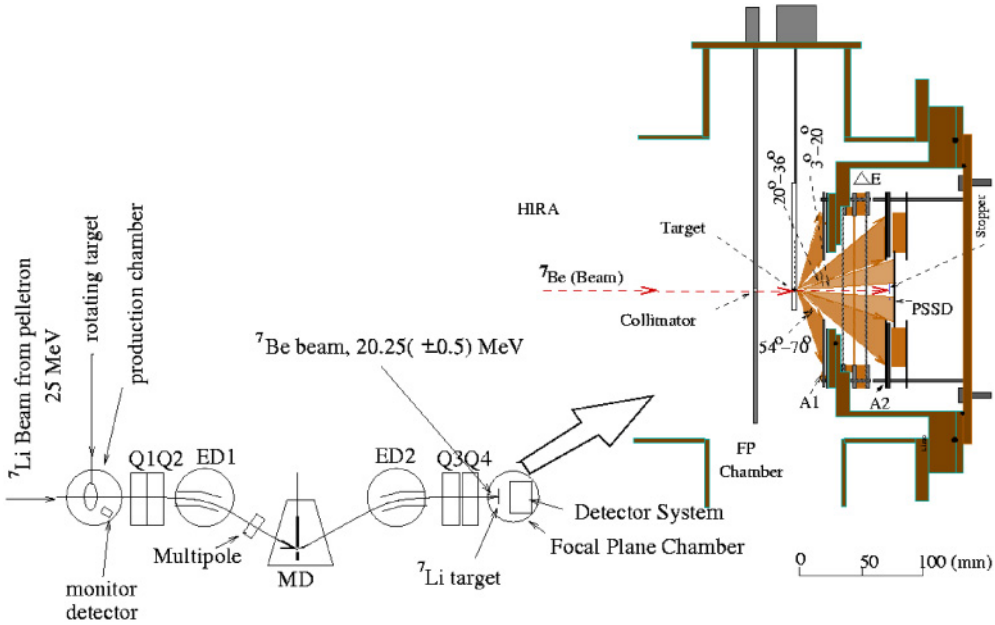

FIG. 1. (Color online) Schematic of the experimental setup; the focal plane arrangement with details of the detector system is shown on right side.

However, scattering involving nuclei with large quadruple moments also shows backward peaking. ^{7}Li has a large ground-state quadrupole moment of 22.5 e fm^2 [17] and thus ground-state reorientation may also contribute toward backward scattering.

With improved experimental conditions the ^{7}Be + ^{7}Li scattering experiment was carried out with the objective of obtaining information about the charge-exchange process. In this paper we report the results of our experiment. The preliminary report may be found in Ref. [18].

The experimental setup and the experimental procedure are described in the next section. Data analysis is presented in Sec. III. In Sec. IV the theoretical background is briefly described. The results are discussed in Sec. V.

II. EXPERIMENT

The experiment was carried out at the radioactive ion beam facility [19] at the Nuclear Science Center, New Delhi. A 25.0-MeV, pulsed ^{7}Li beam from a 15UD Pelletron [20] was made to interact with polypropylene foil to produce a ^{7}Be beam through the inverse kinematic reaction $p(^7\text{Li}, ^7\text{Be})n$. The production foil was mounted on a rotating target system to avoid burning by the beam [21]. A pair of ΔE-E (Si) detectors was mounted in the production chamber to monitor recoil protons. The ^{7}Be beam of energy 20.25 MeV was separated at 0° using the recoil mass spectrometer HIRA (Heavy Ion Reaction Analyzer) [22] operated in new ion optics mode [19]. (The energy chosen was constrained by the capacity of electric dipoles of HIRA.) The intensity of the ^{7}Be beam was 10^4 particles/s and the intrinsic energy spread caused by the energy straggling in the production target was ±0.5 MeV. The intrinsic angular spread of the beam was ±1°. The purity of the beam was 99%.

The ^{7}Li target was prepared by evaporation of ^{7}Li material (99.9% pure) on a thin (10 μg/cm^2) carbon backing. Special care was taken in preparing the target as ^{7}Li is highly hygroscopic. An in-vacuum target transfer system was fabricated for this purpose [23]. The thickness of the target was measured by the energy loss of α particles from an ^{241}Am source and was found to be 628 μg/cm^2. A CD2 (deuterated polypropylene) target of thickness 1 mg/cm^2 was put on one slot of the target ladder and this was used to measure the ^{7}Be + d elastic cross section during the same beam time. While evaporating ^{7}Li on the carbon backing a mask was put in front of the CD2 target. Despite this, some ^{7}Li got deposited on the CD2. The thickness of the ^{7}Li deposited on CD2 was found to be 421 μg/cm^2. This ^{7}Li target was later used to extract the data for ^{7}Be + ^{7}Li elastic scattering at lower energy.

The scattering events were detected in a compact and efficient ΔE(gas)-E(Si) telescope detector system [18,24] in the secondary scattering chamber. This detector system was designed to compensate for the low intensity of the ^{7}Be beam and was operated in kinematic coincidence mode to eliminate the effect of beam halo and other sources of contamination. As shown in Fig. 1, the detector system consisted of two identical position-sensitive Si annular detectors, A1 and A2 (44 × 96 − 500). The front side of the annular detector had 16 rings divided into four quadrants, which gave position (angular) information. The back side of the annular detector was divided into 16 sectors, which provided energy information. The first detector (A1) was placed near the target, at a distance of 17 mm (from the target). The other one (A2) was placed behind a gas

ionization chamber (IC), at a distance of 66 mm from the target. The IC consisted of three parallel grid electrodes with 9 mm separation between them and perpendicular to the beam direction. The first and third grids were grounded, the middle one was kept at positive potential. The angles covered by A1 and A2 were $\theta_{\rm lab} = 54^\circ$–$70^\circ$ and $\theta_{\rm lab} = 20^\circ$–$36^\circ$, respectively, and these were in kinematic coincidence mode for scattering of the ^{7}Be + ^{7}Li system. Detector A2 was also used for particle identification as it formed a telescopic system with the IC. The corresponding particle identification with A1 was possible through kinematic coincidence.

A position-sensitive, large-area (50 mm × 50 mm) Si detector (PSSD) was used to cover forward angles up to 20°. A Ta beam stop of 8 mm diameter was placed in front of the PSSD, in the center, which cast a shadow of 3° about the beam direction on the PSSD and protected it from radiation damage. The performance of the detector system for particle identification and position readout was tested with α particles as well as with a beam using the ^{7}Li + ^{12}C system in an earlier experiment [24]. A charge division technique was employed for position readout of the annular detectors to minimize the requirement of electronics.

The proper alignment of the detector system along with the target with respect to the beam direction was very important for the extraction of angular information. A special mechanical arrangement was used to align the detector system. The detector system and the target were aligned in the beam direction using a theodolite. Since ^{7}Li is highly hygroscopic and could not be exposed to air, the target ladder associated with the in-vacuum target transfer system was aligned before evaporation and then doweled.

An experimental run was taken to verify the alignment of the detector setup for kinematic coincidence using ^{7}Be + d elastic scattering. In this run, forward-scattered ^{7}Be ions were detected in the PSSD alone while the recoiling deuterons were detected in A1. It was found that counts in each quadrant about the beam axis (as constructed in software) of PSSD were equal when gated by deuteron events in A1, hence establishing mutual axis alignment of the detector setup. From the shadow cast by the Ta beam stop on the position spectrum of the PSSD the alignment could be monitored on-line.

The magnetic and electric fields of the HIRA spectrometer were tuned to center the 20.25-MeV ^{7}Be beam on the Ta stopper. This was monitored from the position spectrum of the PSSD. A 5-mm-diameter collimator was put in front of the target to cut down the beam halo and improve the intrinsic angular spread. The target frame was set to 15 mm in diameter to avoid scattering from the frame. Intermittent runs with ^{241}Am αs were also taken to check the consistency of the detector resolution, electronic gain, etc. during the experiment. The α source was mounted on a shaft attached to a linear drive through one of the ports of the focal plane scattering chamber, was put in the beam path when the α runs were taken, and pulled out and kept behind a mask at other times. The pressure of the isobutane gas in the ionization chamber was maintained at 95 ± 0.5 mbar throughout the experiment.

For normalization, a Si surface-barrier detector was mounted on a precision linear drive near the ^{7}Li target position. This detector was periodically brought on the beam axis to count the incident ^{7}Be particles. Recoil proton signals in the monitor detector were also recorded in the event mode. The ratio of recoil protons to ^{7}Be counts was found to be constant indicating that ^{7}Be trajectory remained undisturbed throughout the experiment. Time-of-flight (TOF) spectrum was generated using the timing signal from E(Si) detector as the start and the RF (radio frequency) output signal of the Pelletron beam pulsing system as the stop. This spectrum was used for rejecting unwanted events during off-line analysis. Conventional electronics were used for signal processing and data acquisition was done through CAMAC with indigenous software FREEDOM [25]. The off-line analysis was carried out with CANDLE, a recent version of FREEDOM.

III. DATA ANALYSIS

The data analysis was done carefully with a TOF gate and kinematic coincidence gate to eliminate unwanted background. The ^{7}Li band forming at the two-dimensional spectrum of the IC-A2 corresponds to the ^{7}Be counts in the A1 detector. Measuring both these correlated events in the two detectors makes the measurements more reliable. A Monte Carlo simulation was also done to check the efficiency of the kinematic coincidence between A1 and A2 and it was found that only the inner ring of the back annular detector recorded less than 100% of the scattered and recoiled events. This is because a few particles that were kinematically coincident went beyond the coverage of the first annular detector. The other rings detected the particles with 100% kinematic coincidence efficiency. Since the inner ring of the back annular detector detects the scattered ^{7}Be and the recoil ^{7}Li (which corresponds to the scattered ^{7}Be at 90°), the cross section will increase slightly at the first and last measured angles of the angular distribution of the scattered ^{7}Be.

For an experiment with radioactive ion beams (RIB), because of the intrinsic spread of the beam in energy and angle, the systematic error in the data is more than that with a normal beam. In addition, the statistical error is also more as the beam intensity and hence the reaction yield is low. Moreover, to get the data of our interest in a reasonable period of time we have used relatively thick ^{7}Li target of thickness 628 μg/cm^2, which also contributes toward energy and angular spread. The uncertainty in target thickness determination is 4%. The uncertainty in beam current determination is also about 4%. The uncertainty in solid angle determination is 8%. Total uncertainty is around 16%, but this may be more because of the uncertainty in energy and angle.

IV. THEORETICAL FORMALISM

The theoretical framework adopted for the analysis is briefly mentioned here. The details of the formalism can be found in Ref. [26]. The optical model (OM) analysis was done with an OM potential whose real and imaginary parts depend on the isospin of the interacting nuclei. If two nuclei, A and B with isospin +1/2 and −1/2 (mirror nuclei), respectively, are allowed to interact, the final product may be from direct elastic

scattering or from the charge-exchange reaction between the two. For mirror nuclei such as ^{7}Be + ^{7}Li, the charge-exchange reaction basically happens between the valence proton and the neutron, respectively. It resembles a (p, n) reaction with the interacting nucleons bound to some nucleus (core). If t_a and T_A are the isospin of the projectile and the target, respectively, there are two possible values of the total isospin $T : T_> = T_A + t_a$ (T upper state) and $T_< = T_A - t_a$ (T lower state).

The coupled equations formed explicitly for elastic and charge-exchange channels are

$$\left\{\frac{d^2}{dr^2} - \frac{l(l+1)}{r^2} + \frac{2\mu}{\hbar^2}\left[E_p - U_p^{ij}(r)\right]\right\} = \frac{2\mu}{\hbar^2}U_{pn}(r)f_{ij}^n(r), \tag{1}$$

$$\left\{\frac{d^2}{dr^2} - \frac{l(l+1)}{r^2} + \frac{2\mu}{\hbar^2}\left[E_n - U_n^{ij}(r)\right]\right\} = \frac{2\mu}{\hbar^2}U_{np}(r)f_{ij}^p(r) \tag{2}$$

with

$$U_p^{ij}(r) = \alpha U_<(r) + \beta U_>(r) + V_{\text{s.o.}}(r)a^{ij} + V_{\text{Coul}}(N_A, -1/2), \tag{3}$$

$$U_n^{ij}(r) = \beta U_<(r) + \alpha U_>(r) + V_{\text{s.o.}}(r)a^{ij} + V_{\text{Coul}}(N_A - 1, 1/2), \tag{4}$$

$$U_{pn}(r) = U_{np}(r) = (\alpha\beta)(U_>) - (U_<), \tag{5}$$

where

$$\alpha = \frac{(T_A + N_A)}{(2T_A + 1)}, \tag{6}$$

$$\beta = \frac{(T_A - N_A + 1)}{(2T_A + 1)}, \tag{7}$$

$$a^{ij} = 1/2[j(j+1) - l(l+1) - 3/4]. \tag{8}$$

Here, N_A is the Z component of isospin of the target. The $U_>$(r) and $U_<$(r) are defined as

$$U_>(r) = U_o(T_>)f_>(r) + \frac{T_A}{2A}U_1(T_>)g_>(r), \tag{9}$$

$$U_<(r) = U_o(T_<)f_<(r) + \frac{(T_A + 1)}{2A}U_1(T_<)g_<(r), \tag{10}$$

where f_T(r) and g_T(r) are the radial form factors. Similar forms of the potentials for the imaginary part are used. However, $|W_<| > |W_>|$ according to isospin conservation. Again from the symmetry energy and Pauli exclusion principle, $|U_>| > |U_<|$. Solving Eq. (3) one can get the charge-exchange reaction cross section along with the elastic scattering cross section. Since the final products are indistinguishable with respect to exit reaction channel, the total cross section for the final products is obtained by the coherent addition of the scattering amplitudes from both channels; that is,

$$f(\theta, \phi) = f_d(\theta, \phi) + f_{\text{ce}}(\pi - \theta, \pi + \phi), \tag{11}$$

where $f(\theta, \phi)$ is the total scattering amplitude, $f_d(\theta, \phi)$ is the direct elastic scattering amplitude, and $f_{\text{ce}}(\pi - \theta, \pi + \phi)$ is the charge-exchange scattering amplitude.

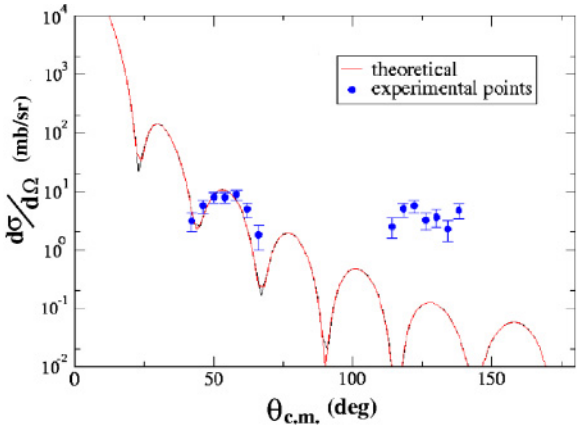

FIG. 2. (Color online) The experimental data and the elastic calculation with Snoopy.

V. RESULTS AND DISCUSSION

A. Isospin-dependent potential

A fit to the experimental elastic cross sections was first tried with the OM potential without isospin dependence with the help of the OM code Snoopy [27]. The forward-angle data were fitted well with this, but the code failed to fit the data at backward angles (in c.m.). The backward-angle data were higher than values from the theoretical calculation. Figure 2 shows the pure elastic calculation with Snoopy.

The isospin-dependent terms were then included in the OM potential and both the forward- and backward-angle cross sections were reasonably well fitted as shown in Fig. 3. The best-fit OM parameters are given in Table I.

Here a spin-orbit term was also included with $U_{\text{s.o.}} = 7.0$ MeV, $r_{\text{s.o.}} = 1.211$ fm, and $a_{\text{s.o.}} = 0.621$ fm. However, the spin term is not treated exactly here. The spin of ^{7}Be and ^{7}Li is 3/2, but in the analysis, spins were set to 1/2 because of the limitation in the program. The effect of this on the cross-section data is expected to be small. The initial parameters were taken from Ref. [28], from the system ^{7}Li + ^{7}Li at 17 MeV. In Fig. 4 the dashed double-dotted curve is for charge exchange

TABLE I. The best-fit OM parameters obtained in the isospin coupled approach. (In W_d, d stands for surface potential.)

U_0	r_0	a_0	$W_{d<}$	$W_{d>}$	r_w	a_w	U_1	r_1	a_1
110	1.211	0.621	47.0	14.0	1.402	0.219	30.0	1.211	0.621

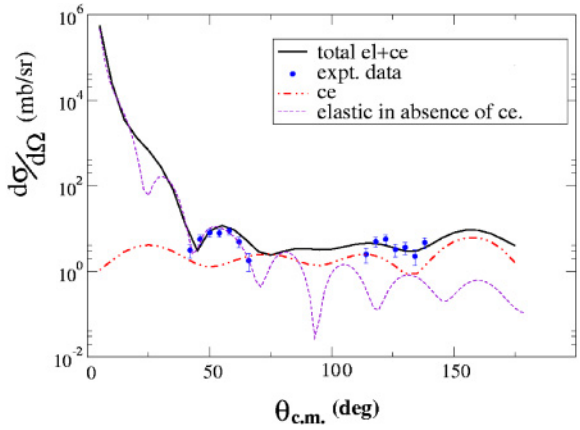

FIG. 3. (Color online) The experimental angular distribution data (filled circles) and isospin coupled (solid curve) and isospin noncoupled (dashed curve) theoretical fits. The dashed double-dotted curve is the charge-exchange contribution in the isospin coupled analysis.

and the solid line is the total (elastic plus charge exchange) cross section. The dashed curve is the elastic scattering cross section in the absence of charge exchange.

In Fig. 4, the normalized cross section in terms of ratio to Rutherford cross section is shown for both at $E_{\text{c.m.}} =$ 9.87 and 8.87 MeV. Here solid curves are from the isospin coupled calculation and the dashed curves are from the nonisospin coupled calculation. At $E_{\text{c.m.}} = 8.87$ MeV, the data at backward angles were well fitted, but not at the forward angles.

However, the inelastic channel, which is also open at this energy, has not been taken into consideration. The first excited state of ^{7}Be is at 0.429 MeV and that of ^{7}Li is at 0.477 MeV. The beam energy spread and the energy straggling in the target itself are greater than these values. A coupled-channel calculation with elastic, inelastic, and charge exchange should be done to determine the actual contribution from the coupling

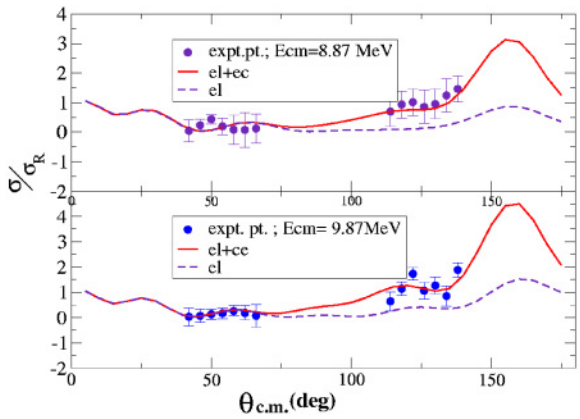

FIG. 4. (Color online) Comparison of the experimental data of ^{7}Be + ^{7}Li at $E_{\text{c.m.}} = 9.87$ and 8.87 MeV and the theoretical fitting with isospin-dependent and isospin-independent OM potentials. The solid curves obtained are from the isospin coupled approach and the dashed curves are obtained from the isospin-independent potentials.

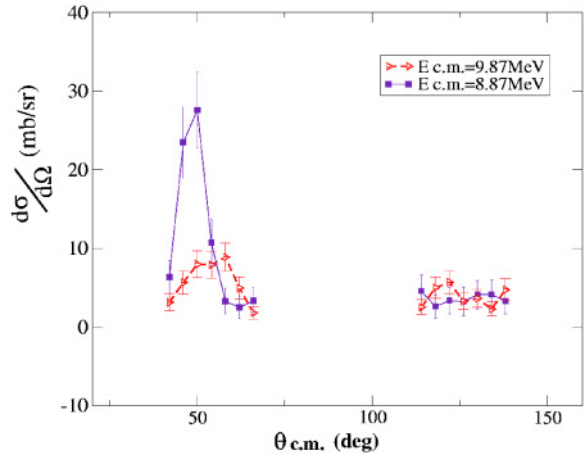

FIG. 5. (Color online) Experimental angular distributions of ^{7}Be + ^{7}Li at $E_{\text{c.m.}} = 9.87$ and 8.87 MeV.

of the channels. Moreover, as both ^{7}Be and ^{7}Li have high breakup probability, with breakup thresholds of 1.47 and 2.47 MeV, respectively, breakup channels should also be taken into account in coupled-channel formalism. At present, such a calculation is beyond the scope of this work.

Another interesting result was obtained at $E_{\text{c.m.}} =$ 8.87 MeV. The behavior of the experimental data at the backward angle is similar to that at $E_{\text{c.m.}} = 9.87$ MeV, but at forward angles of around 50° in the c.m. there is a well-defined peak (Fig. 5). At $E_{\text{c.m.}} = 9.87$ MeV also, around this angle, there is an indication of a broad peak, which is not as clear as that at $E_{\text{c.m.}} = 8.87$ MeV.

Unfortunately, no data could be taken at lower energies because of limited beam time to confirm whether or not the peak is due to resonance scattering.

B. Ground-state reorientation

Since ^{7}Be and ^{7}Li both have large quadrupole moments, a coupled-channel calculation with ground-state reorientation

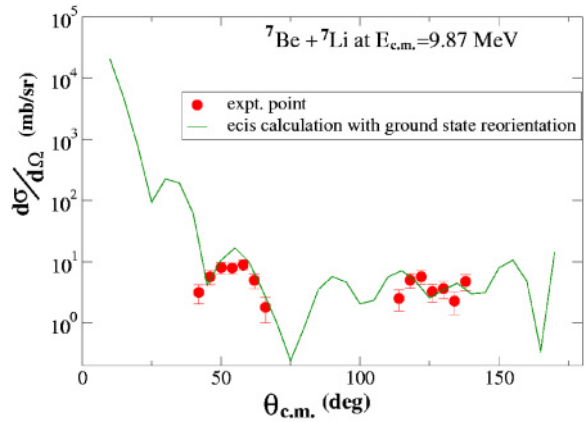

FIG. 6. (Color online) Experimental angular distribution of ^{7}Be +^{7}Li at $E_{\text{c.m.}} = 9.87$ MeV and a theoretical fit with couple channels calculation (ECIS).

was also performed with the code ECIS [29]. The deformation parameter of ^{7}Li is taken as 0.50 [30]. With slight variation of OM parameter data, both regions could be fitted well, as shown in Fig. 6. r_o was changed to 1.311 fm from 1.211 fm and W_o was changed to 24.5 MeV from 30.5 MeV.

VI. CONCLUSION

In this paper, we have reported the measurement of angular distribution of ^{7}Be + ^{7}Li. The experimental difficulties encountered in the study of mirror nuclei (^{7}Be + ^{7}Li) scattering with a radioactive ^{7}Be beam have been described and remedial steps were taken are briefly stated. The experiment was designed to perform the measurement as cleanly as possible. However, because it involves a radioactive ion beam systematic and statistical errors are much greater than the corresponding ones with a stable beam. The experiment was done at $E_{\text{c.m.}} = 8.87$ and 9.87 MeV. In the evaluation of the elastic data, the kinematic coincidence and the TOF condition helped effectively to remove irrelevant data. The elastic scattering angular distribution for ^{7}Be + ^{7}Li shows a behavior different from that of an asymmetric system. The angular distribution rises higher at backward angles (c.m.) than predicted for any direct elastic cross section. The increase in cross sections at backward angles is thought to be due to contributions from charge exchange along with the direct elastic process. Data-fitting with isospin-dependent real and imaginary potentials, similar to the Lane potential [31], is able to explain this behavior the angular distribution at backward angles. The Lane potential also implies the presence of a charge-exchange reaction. Assuming that charge exchange is a perturbation in the dominating elastic cross section allows one to solve the coupled equation for elastic and charge exchange to get the fitting. The code used for analysis was the modified TWAVE code originally written by S. Cotanch [26,32].

A coupled-channel calculation with ground-state reorientation could also fit the data well.

Another unusual result was obtained for $E_{\text{c.m.}} = 8.87$ MeV. A well-defined peak was observed in the forward angle data. Because of lack of data for the ^{7}Be + ^{7}Li system in this energy region, the origin of the peak could not be interpreted.

ACKNOWLEDGMENTS

We thank Prof. G. K. Mehta, Prof. C. V. K. Baba, Dr. A. Roy, Prof. R. Singh, Dr. S. Kailas, Dr. V. M. Datar, Dr. A. Navin, Dr. R. K. Bhowmik, Dr. A. K. Sinha, Dr. Sumit Mukharjee, and Prof. J. D. Fox for useful guidance and suggestions; E. T. Subramaniam for support in data acquisition; and the accelerator crew for delivering the required primary beam. S. Barua wishes to thank the Council for Scientific and Industrial Research, New Delhi, for financial assistance.

[1] G. M. Temmer, Phys. Lett. **1**, 10 (1962).
[2] W. von Oretzen, Nucl. Phys. **A148**, 529 (1970).
[3] A. Gobbi *et al*., Nucl. Phys. **A112**, 537 (1968).
[4] A. Kuehner *et al*., Phys. Rev. **131**, 1245 (1963).
[5] B. Imanishi and W. von Oretzen, Phys. Rep. **155**, 29 (1987).
[6] M. A. Nagarajan and J. P. Vary, Phys. Rev. C **43**, 281 (1991).
[7] G. R. Satchler, in *Isospin in Nuclear Physics*, edited by D. H. Wilkinson (North-Holland Publishing Company, Amsterdam, 1969), p. 391.
[8] P. E. Hodgson, *The Nucleon Optical Model* (World Scientific, London, 1994).
[9] P. E. Hodgson, *Nuclear Reactions and Nuclear Structure* (Clarendon Press, Oxford, 1971).
[10] A. D. Bacher, R. J. Spiger, and T. A. Tombrello, Nucl. Phys. **A119**, 481 (1968).
[11] E. Lienard, D. Baye, Th. Delbar, P. Descouvemont, P. Duhamel, W. Galster, M. Kurokawa, P. Leleux, I. Licot, P. Lipnik, C. Michotte, T. Motobayashi, A. Ninane, J. M. Sparenberg, J. Vanhorenbeeck, and J. Vervier, Phys. Rev. C **54**, 2477 (1996).
[12] R. N. Boyd, M. S. Islam, G. Kolnicki, M. Farrell, T. F. Wang, K. E. Sale, and G. J. Mathews, in *The Proceedings of 1st International Conference on Radioactive Ion Beams 16–18 Oct (1989) at Berkeley, CA* (World Scientific, London, 1989), p. 311.
[13] A. T. Kruppa, M. A. Nagarajan, and J. P. Vary, Phys. Rev. C **47**, R451 (1993).
[14] N. Nose-Togawa and K. Kume, Phys. Rev. C **59**, 2162 (1999) and references therein.
[15] M. D. Cooper, H. W. Baer, R. Bolton, J. D. Bowman, F. Cverna, N. S. P. King, M. Leitch, J. Alster, A. Doron, A. Erell, M. A. Moinester, E. Blackmore, and E. R. Siciliano, Phys. Rev. Lett. **52**, 1100 (1984).
[16] F. Irom *et al*., Phys. Rev. C **31**, 1464 (1985).
[17] V. Hnizdo, K. W. Kemper, and J. Szymakowski, Phys. Rev. Lett. **46**, 590 (1981).
[18] S. Barua, J. J. Das, A. Jhingan, T. Varughese, N. Madhavan, K. Kalita, S. Verma, P. Sugathan, B. Bhattacharjee, S. K. Datta, and K. Baruah, Nucl. Phys. **A746**, 467c (2004).
[19] J. J. Das, P. Sugathan, N. Madhavan, B. Kumar, T. Varughese, P. V. M. Rao, and A. K. Sinha, J. Phys. G **24**, 1371 (1998).
[20] G. K. Mehta and A. P. Patro, Nucl. Instrum. Methods A **268**, 334 (1988).
[21] T. Varughese, J. J. Das, N. Madhavan, P. Sugathan, P. V. Madhusudhana Rao, A. Jhingan, S. Nath, A. K. Sinha, and J. Zacharias, Nucl. Instrum. Methods A **521**, 143 (2004).
[22] A. K. Sinha, N. Madhavan, J. J. Das, P. Sugathan, D. O. Kataria, A. P. Patro, and G. K. Mehta, Nucl. Instrum. Methods A **339**, 543 (1994).
[23] S. Barua, B. Bhattacharjee, K. Barua, T. Varughese, A. Jhingan, J. J. Das, P. Sugathan, S. Nath, P. V. Madhusudhana Rao, N. Madhavan, S. K. Datta, S. Verma, and K. Kalita, DAE Symposium on Nuclear Physics, Tirunelveli, India, 468 (2002).
[24] A. Jhingan, S. Barua, J. J. Das, T. Varughese, P. Sugathan, N. Madhavan, K. Kalita, and S. Verma, Nucl. Instrum. Methods Phys. Res. A **539**, 269 (2005).
[25] B. P. Ajithkumar, E. T. Subramanium, and R. K. Bhowmick, in Proceedings of SANAI98, Bombay, February (1998).

[26] S. Cotanch and D. Robson, Nucl. Phys. **A209**, 301 (1973).
[27] P. Schwandt, H. O. Meyer, W. W. Jacobs, A. D. Bacher, S. E. Vigdor, M. D. Kaitchuck, and T. R. Donoghue, Phys. Rev. C **26**, 55 (1982).
[28] A. M. Bachmann *et al*., Z. Phys. A **346**, 47 (1993).
[29] J. Raynal, International Atomic Energy Agency Rep. No. IAEA-SMR-918, 1972, p. 281.
[30] A. T. Rudchik, Val. M. Pirnak, A. Budzanowski, A. Szczurek, V. K. Chernievsky, L. Gowacka, S. Kliczewski, E. I. Koshchy, A. V. Mokhnach, R. Siudak, I. Skwirczyska, J. Turkiewicz, and V. A. Ziman, Nucl. Phys. **A700**, 25 (2002).
[31] A. M. Lane, Nucl. Phys. **35**, 676 (1962).
[32] S. Cotanch, Technical Report, Tandem Accelerator Laboratory, Florida State University, 1973 (unpublished).